Redox Biology 64 (2023) 102790

Contents lists available at ScienceDirect

Redox Biology

journal homepage: www.elsevier.com/locate/redox

Loss of cytochrome P450 (CYP)1B1 mitigates hyperoxia response in adult mouse lung by reprogramming metabolism and translation

Sandra L. Grimm [a,b,c,1], Rachel E. Stading [d,1], Matthew J. Robertson [a], Tanmay Gandhi [a], Chenlian Fu [a,e], Weiwu Jiang [d], Guobin Xia [d], Krithika Lingappan [f], Cristian Coarfa [a,b,c,**,2], Bhagavatula Moorthy [c,d,2,*]

[a] Dan L Duncan Comprehensive Cancer Center, Baylor College of Medicine, Houston, TX, USA
[b] Dept. of Molecular and Cellular Biology, Baylor College of Medicine, Houston, TX, USA
[c] Center for Precision Environmental Health, Baylor College of Medicine, Houston, TX, USA
[d] Division of Neonatology, Department of Pediatrics, Baylor College of Medicine and Texas Children's Hospital, Houston, TX, USA
[e] Mathematical and Computational Biology, Harvey Mudd College, CA, USA
[f] Division of Neonatology at Children's Hospital of Philadelphia, USA

ARTICLE INFO

Keywords:
Hyperoxia
Cytochrome P450
CYP1B1
Bronchopulmonary dysplasia
Lung
Oxidative stress

ABSTRACT

Oxygen supplementation is life saving for premature infants and for COVID-19 patients but can induce long-term pulmonary injury by triggering inflammation, with xenobiotic-metabolizing CYP enzymes playing a critical role. Murine studies showed that CYP1B1 enhances, while CYP1A1 and CYP1A2 protect from, hyperoxic lung injury. In this study we tested the hypothesis that *Cyp1b1*-null mice would revert hyperoxia-induced transcriptomic changes observed in WT mice at the transcript and pathway level. Wild type (WT) C57BL/6J and *Cyp1b1*-null mice aged 8–10 weeks were maintained in room air (21% O_2) or exposed to hyperoxia (>95% O_2) for 48h. Transcriptomic profiling was conducted using the Illumina microarray platform. Hyperoxia exposure led to robust changes in gene expression and in the same direction in WT, *Cyp1a1*-, *Cyp1a2*-, and *Cyp1b1*-null mice, but to different extents for each mouse genotype. At the transcriptome level, all *Cyp1*-null murine models reversed hyperoxia effects. Gene Set Enrichment Analysis identified 118 hyperoxia-affected pathways mitigated only in *Cyp1b1*-null mice, including lipid, glutamate, and amino acid metabolism. Cell cycle genes *Cdkn1a* and *Ccnd1* were induced by hyperoxia in both WT and *Cyp1b1*-null mice but mitigated in *Cyp1b1*-null O_2 compared to WT O_2 mice. Hyperoxia gene signatures associated positively with bronchopulmonary dysplasia (BPD), which occurs in premature infants (with supplemental oxygen being one of the risk factors), but only in the *Cyp1b1*-null mice did the gene profile after hyperoxia exposure show a partial rescue of BPD-associated transcriptome. Our study suggests that CYP1B1 plays a pro-oxidant role in hyperoxia-induced lung injury.

1. Introduction

Oxygen supplementation is a life-saving treatment used for patients with a multitude of diseases [1]. However, excess oxygen supplementation not only causes acute, but also chronic, lung damage [2]. Hyperoxic lung injury occurs when excess oxygen triggers inflammatory processes resulting in damage to pulmonary tissues [3]. The importance of understanding the underlying mechanisms in hyperoxia-mediated lung injury has increased tremendously in the past few years as more patients have required oxygen supplementation for the treatment of acute respiratory distress syndrome (ARDS) following COVID-19 infections [4]. Another group at risk of hyperoxic lung injury due to supplemental oxygen requirements are premature infants, who could develop bronchopulmonary dysplasia (BPD) [5], the most common morbidity associated with preterm birth.

Hyperoxic lung injury caused by supplemental oxygen may

* Corresponding author. Division of Neonatology, Department of Pediatrics, Baylor College of Medicine and Texas Children's Hospital, Houston, TX, USA.
** Corresponding author. Dan L Duncan Comprehensive Cancer Center, Baylor College of Medicine, Houston, TX, USA.
E-mail addresses: coarfa@bcm.edu (C. Coarfa), bmoorthy@bcm.edu (B. Moorthy).
[1] First authors contributed equally.
[2] Senior authors contributed equally.

https://doi.org/10.1016/j.redox.2023.102790
Received 17 April 2023; Received in revised form 5 June 2023; Accepted 15 June 2023
Available online 16 June 2023

necessitate even more oxygen, further contributing to the lung injury. Thus, the treatment for the problem enhances the problem, creating a vicious cycle of injury. The optimal oxygenation level that may satisfy the patient's oxygen requirements while minimizing the pulmonary tissue damage is challenging to implement clinically [6,7]. To improve management of patients requiring supplemental oxygen, a better understanding of the underlying mechanisms through which hyperoxia perpetuates lung injury is needed. Altering or mitigating the adverse effects of these mechanisms may provide us with a solution in which patients may be given the required oxygen supplementation without the risk of hyperoxic lung injury.

One such mechanism shown to play a critical role in hyperoxic lung injury involves the xenobiotic-metabolizing cytochrome 450 (CYP) enzymes [8]. CYP enzymes have been studied extensively for their contribution in drug and xenobiotic metabolism. This family of enzymes is found throughout the body, most significantly in the liver and lungs [9]. These phase-I oxidative enzymes may contribute to oxidative stress due to production of reactive oxygen species (ROS), resulting in lipid peroxidation and DNA damage that may perpetuate hyperoxic lung injury [8]. Interestingly, CYP enzymes also play roles in ROS detoxification [10].

Three commonly studied CYP enzymes have been linked to hyperoxic lung injury, specifically the CYP1A1, CYP1A2, and CYP1B1 enzymes [3,8,11]. While CYP1A1 and 1B1 are constitutively present in lung, CYP1A2 is predominantly expressed in liver. Murine studies have shown that the CYP1B1 enzyme may contribute to hyperoxic lung injury as *Cyp1b1*-null mice had reduced lung injury compared to WT mice upon exposure to hyperoxia [10]. In contrast, studies have shown that *Cyp1a1*-null and *Cyp1a2*-null mice experience more significant lung injury compared to WT mice in hyperoxic environments [11]. Therefore, the CYP1A1 and CYP1A2 enzymes attenuate, while CYP1B1 potentiates, hyperoxic lung injury [10].

Although prior studies established the relationship between these enzymes and lung injury, the underlying mechanisms remain unclear. Because of the various interconnected pathways that these CYP enzymes influence, these mechanisms are difficult to untangle. We recently reported transcriptomic and proteomic profiling of lung samples of WT, *Cyp1a1*-null, and *Cyp1a2*-null mice exposed to hyperoxia [11]; after hyperoxic injury, DNA repair was induced in WT but suppressed in both mutants, while early estrogen response was suppressed in WT but induced in both mutants; apoptosis was suppressed in WT and *Cyp1a1*-null but induced in *Cyp1a2*-null mice. To analyze the mechanisms by which CYP1B1 contributes to hyperoxic lung injury, we exposed WT and *Cyp1b1*-null mice to hyperoxia (95% O_2) treatment for 48 h and subjected the lung tissues to transcriptomics microarray and Reverse Phase Protein Array (RPPA) analysis. We sought to identify key pathways altered by hyperoxia in *Cyp1b1*-null but not in *Cyp1a1*-or *Cyp1a2*-null mice as well as to examine which of the lung hyperoxia signatures associated with various pathologic lung conditions: BPD, lung cancer, acute respiratory distress syndrome (ARDS), and idiopathic pulmonary fibrosis (IPF). Fig. 1 demonstrates the overarching analytical approach deployed in this research. As the phenotype observed in *Cyp1b1*-null mice has been opposite to that in mice lacking *Cyp1a1* or *Cyp1a2,* we speculated that CYP1B1 plays a pro-oxidant role in oxygen injury. Thus, we hypothesize that unique molecular pathways in *Cyp1b1*-null mice under hyperoxic conditions mitigate lung injury.

2. Materials and methods

2.1. Animals

Male mice were used for all studies. C57BL/6J wild type (WT) mice were purchased from Charles River Laboratories (Wilmington, Delaware). *Cyp1a1*-null and *Cyp1a2*-null mice, on a C57BL/6J background, have been previously described [11]. *Cyp1b1*-null mice, on a C57BL/6J background, were generated by Dr. Frank J. Gonzalez and have been previously described [12]. The Institutional Animal Care and Use Committee of Baylor College of Medicine approved the study (Protocol No: AN-907), which was performed in accordance with federal guidelines for the humane care and use of laboratory animals. Animals were maintained at the Feigin Center animal facility at Baylor College of Medicine (Houston, Texas). Animals were kept under a 12-h day/night light cycle and were provided purified tap water and food (Purina Rodent Lab Chow 5001 from Purina Mills, Inc., Richmond, Indiana) *ad libitum*. Mice used in these experiments were between 8- and 10-weeks old.

2.2. Hyperoxia exposure and tissue harvesting

Male mice were randomly selected for each treatment group and were maintained in room air (21% O_2) as a control group or exposed to hyperoxia (>95% O_2) using pure O_2 at 5 L/min for 48h, in a sealed Plexiglass chamber. The oxygen concentration in the plexiglass chamber was monitored by an oxygen analyzer (Getronics, Kenilworth, New Jersey). Following hyperoxia exposure, animals were anesthetized with sodium pentobarbital (200 mg/kg i.p.) and euthanized by exsanguination while under deep anesthetization. Lung tissues were collected and snap frozen at −80 °C for future analysis.

2.3. RNA isolation

RNA extraction and quality control were performed as described previously, with minor modifications [11]. Three biological replicates per experimental group were used for these analyses. Total RNA from

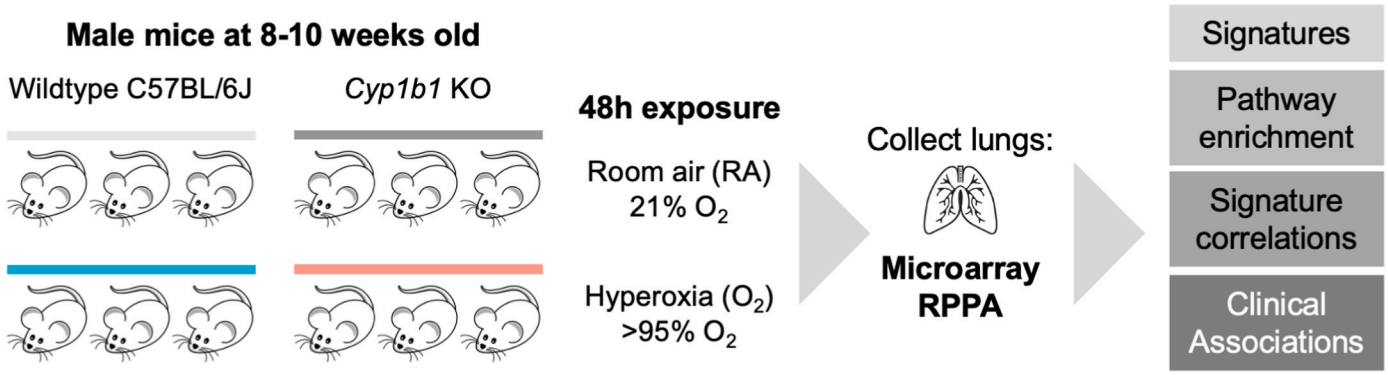

Fig. 1. Experimental design. Wildtype (WT) C57BL/6J mice and *Cyp1b1*$^{-/-}$ (*Cyp1b1*-null) mice were exposed for 48 h to either room air (RA) or hyperoxia (O_2). Lungs were collected and assayed for gene expression using microarray or for protein expression using Reverse Phase Protein Array (RPPA) platforms. We evaluated the transcriptional phenotype of *Cyp1b1*-null mice using gene signatures, enriched pathways, gene signature correlations, and clinical associations with potential lung disease endpoints.

frozen lung samples was isolated using the miRNeasy kit as per the manufacturer's standard protocols (Qiagen, Valencia, CA, USA). Sample RNA concentration was measured using a Nanodrop-8000 (Thermo Scientific, Wilmington, DE, USA) and quality checks were done using the NanoDrop spectrophotometer and the Agilent Bioanalyzer. The 260/280 and 260/230 ratios needed to be greater than 1.8 to meet RNA quality control. Additionally, RNA samples needed an RNA Integrity Number (RIN) value between 7 and 10.

2.4. Microarray transcriptomics analysis

RNA profiling using Illumina Gene Expression MouseWG-6 v2.0 Expression BeadChip Kit was performed at the Laboratory for Translational Genomics at Baylor College of Medicine as previously described [11]. Preprocessing of the microarray data, including quality control, background adjustment, and variance stabilization, was performed using the Lumi package [13] implemented in the R statistical system. A transcript was considered 'detected' at a p-value cutoff of <0.01. Significantly changed probes were determined using the limma package [14] as implemented in the R statistical system, with significance achieved for fold change exceeding 1.5x and FDR-adjusted p-value<0.05. Differentially expressed probes were depicted as heatmaps using the heatmap package implemented in the R statistical system. Enriched pathways were determined using the Gene Set Enrichment Analysis (GSEA) method [15], with significance achieved at FDR<0.25. Selected genes were validated by qRT-PCR, as previously described [11].

2.5. Reverse phase protein array (RPPA)

Frozen whole lung tissues were homogenized with a T25 Ultra-Turrax (Janke & Kunkel) at 8000 rpm in lysis buffer (1% Triton X-100, 50 mM HEPES pH 7.4, 150 mM NaCl, 1.5 mM $MgCl_2$, 1 mM EGTA, 100 mM NaF, 10 mM Na pyrophosphate, 1 mM Na_3VO_4, 10% glycerol, containing freshly added protease and phosphatase inhibitors from Roche Applied Science Cat. # 05056489001 and 04906837001, respectively). The volume of lysis buffer was 1 ml per 40 mg of tissue. After centrifugation to remove debris, the supernatant was collected, protein concentration was measured, and the lysates were diluted to 1.5 mg/ml using lysis buffer. Three parts lysate were added to one part 4x SDS sample buffer (40% Glycerol, 8% SDS, 0.25 M Tris.HCL pH 6.8, 10% ß-mercaptoethanol), boiled for 5 min, and stored at −80 °C. Reverse phase protein array analysis (RPPA) was performed in the Functional Proteomics RPPA core facility at the MD Anderson Cancer Center as previously described [11]. In summary, tissue lysates were serially diluted by increasing two-fold ratios for 5 consecutive dilutions (ranging from undiluted to 1:16 dilution) and arrayed on nitrocellulose coated slides in an 11 × 11 format. Samples were assayed with antibodies by tyramide-based signal amplification approach and visualized using DAB colorimetric reaction. Slides were scanned on a flatbed scanner to generate 16-bit tiff image. Spots from tiff images were identified and the density was quantified by Array-Pro Analyzer. The protein expression was normalized by integrating all dilution curves for all samples and all antibodies, using the Supercurve algorithm [16].

2.6. Analysis of human cohorts using murine gene signatures

As previously reported [17], we computed activity scores for murine gene signatures in human cohorts using summed z-scores. Briefly, in a human cohort each gene was transformed to z-scores. For a murine gene signature and for every specimen, z-scores of increased genes were added, and z-scores of decreased genes were subtracted, computing a summed z-score. Human orthologs of mouse genes were determined using the BioMart repository [18]. We determined correlations of activity scores in human cohorts using the Python scientific library, with significance achieved at $p < 0.05$. For human cohorts with control and case specimens, we used a numerical encoding of the control/case, then performed Pearson correlation analysis between signature scores and numerically encoded clinical variables; significance was achieved for $p < 0.05$. Signature correlation results were plotted using GraphPad Prism.

For gene signature correlation, the following lung cohorts were downloaded and used: lung explant controls GSE151052, TCGA Lung Adenocarcinoma [19], TCGA Lung squamous carcinoma [20], and normal GTEx lungs [21]. Bronchopulmonary dysplasia (BPD) blood transcriptomics from newborns were downloaded using the dataset GSE32472 [22]. ARDS patients' blood transcriptomics were downloaded using the dataset GSE32707 [23]. Idiopathic pulmonary fibrosis (IPF) transcriptomics datasets used included GSE93606 [24], GSE53845 [25], GSE35145 [26], GSE24206 [27], and GSE110147 [28].

2.7. Statistical analysis

Statistical significance was achieved using a parametric two-tailed unequal variance Student's t-test, with significance being achieved at $p < 0.05$.

3. Results

3.1. Disruption of Cyp1b1 mitigated the murine response to hyperoxia

Using transcriptome microarray analysis, we determined the hyperoxia exposure response of WT and *Cyp1b1*-null mice (Fig. 2A). Whereas a robust hyperoxia response was observed in both WT (with 638 genes increased and 565 genes decreased) and *Cyp1b1*-null mice (with 489 induced and 424 decreased genes), minimal differences were detected between WT and *Cyp1b1*-null mouse lungs under either normoxia (9 induced and 28 decreased genes) or hyperoxia (28 induced and 60 decreased genes) conditions. In a previous publication, our group reported signatures of hyperoxia exposure for other murine models genetically modified to delete Cytochrome P450 genes, specifically *Cyp1a1*-null and *Cyp1a2*-null mice [11]. To compare the relationship between gene signatures, while accounting for unclear gene-gene relationships, we used the analytical tool of Pearson Correlation based on gene activity scores over transcriptome profiles of lungs from human cohorts, a computationally established methodology [17,29,30]. Specifically, we computed gene signature summed z-scores independently over several transcriptomic cohorts of normal human lungs, including explants, normal adjacent tissues compiled by The Cancer Genome Atlas (TCGA) for lung adenocarcinoma (LUAD) [19], lung squamous carcinoma (LUSC) [20], and also lungs compiled by the Genotype-Tissue Expression (GTEx) project [21] (Fig. 2B). Interestingly, we determined that hyperoxia transcriptomic responses of WT, *Cyp1a1*-null, *Cyp1a2*--null, and *Cyp1b1*-null mice were highly correlated, with a Pearson Correlation Coefficient in the range 0.93–0.98 ($p < 0.05$). Strikingly, signatures comparing the hyperoxia exposure in genetically modified mice *Cyp1a1*-null, *Cyp1a2*-null, and *Cyp1b1*-null with the hyperoxia exposure in WT mice revealed a negative correlation in multiple cohorts with the canonical (WT) hyperoxia response ($p < 0.05$) (Fig. 2B). For each of the CYP mutant mice, we observed negative correlations over the GTEx human lungs between the WT hyperoxia response and the mutant hyperoxia to WT hyperoxia signatures, ranging from −0.50 to −0.65 ($p < 0.05$) (Fig. 2C), suggesting that loss of these CYP enzymes might reverse some of the effects of hyperoxia through commonly regulated genes.

3.2. Hyperoxic damage is attenuated in Cyp1b1-null mice via a coordinated metabolic program

We have shown that hyperoxia exposure led to correlated transcriptomic responses in WT mice and in null models for *Cyp1a1*, *Cyp1a2*, and *Cyp1b1* (Fig. 2B). A similar observation was substantiated by enriched pathway profiles by GSEA using the Gene Ontology Biological

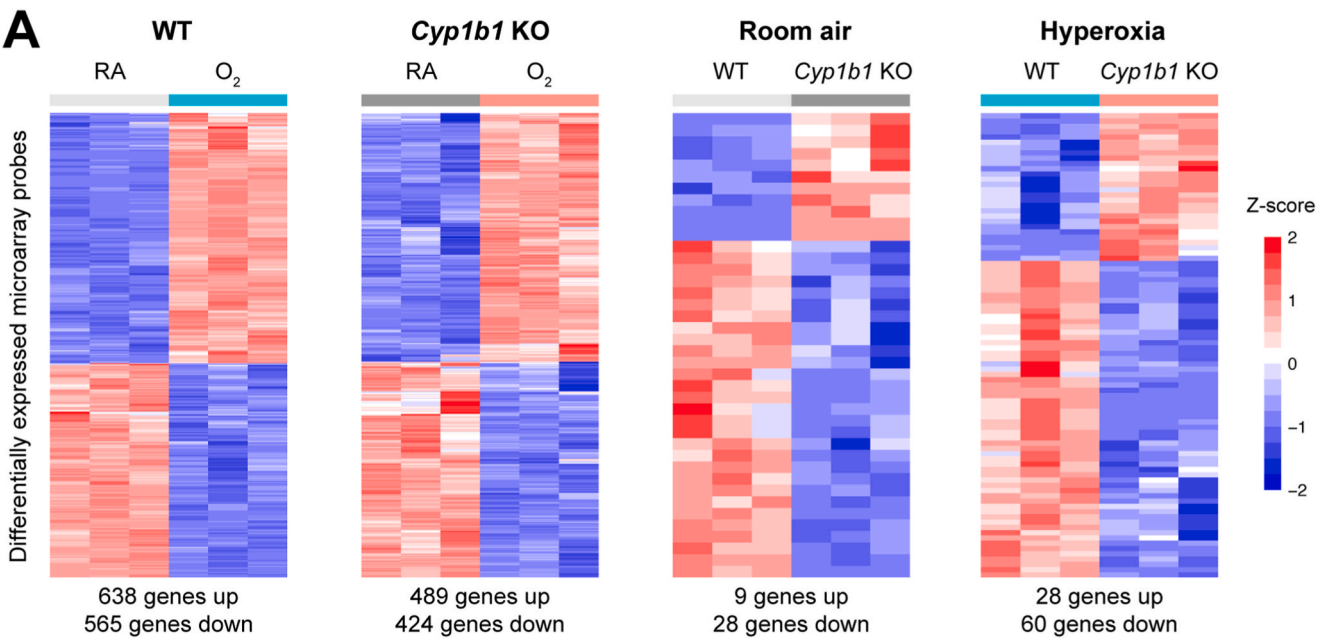

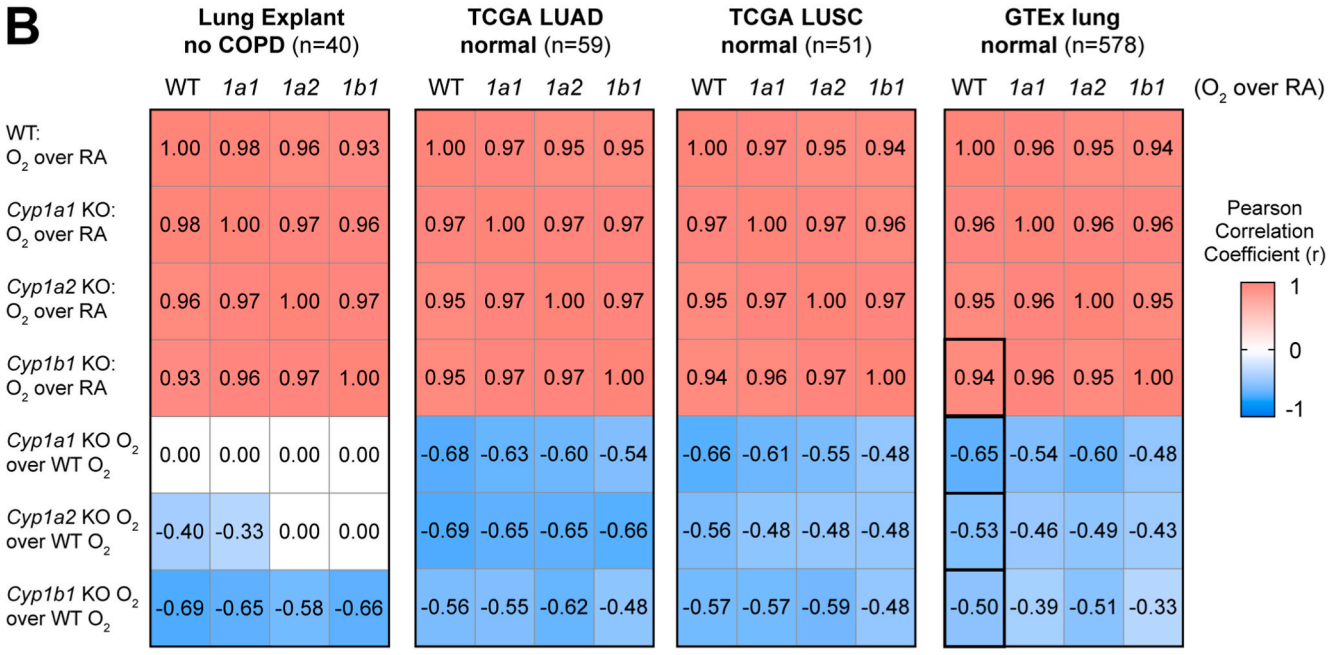

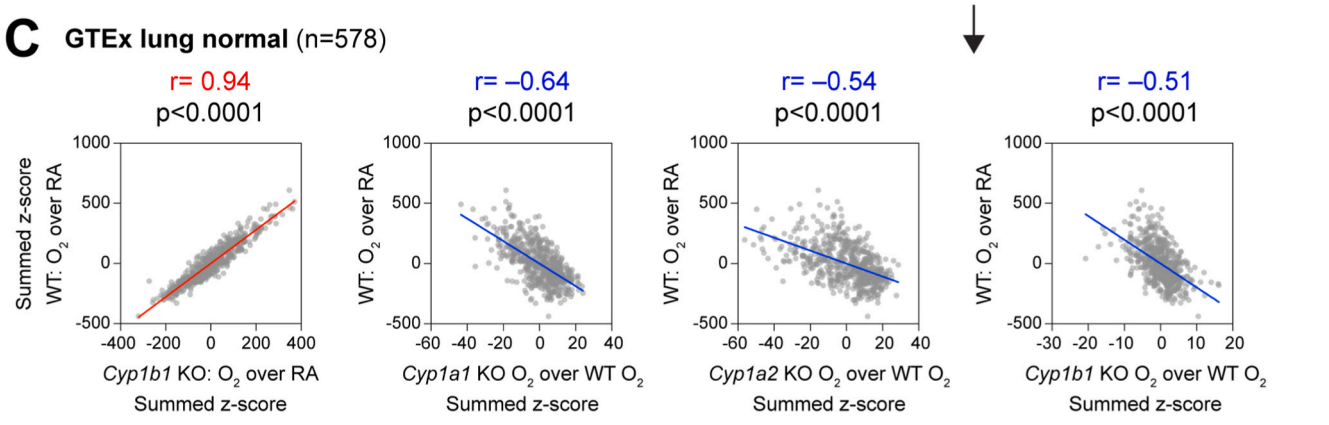

(caption on next page)

Fig. 2. *Cyp1b1*-null mice exhibited a robust hyperoxia exposure response and potentially mitigated the wildtype response. A. Heatmaps of differentially expressed microarray probes, assessing hyperoxia response in WT or *Cyp1b1*-null mice (left) or differences between WT and *Cyp1b1*-null mice under either normoxia (RA) or hyperoxia (O_2) conditions (right). The number of differentially expressed genes is listed below each heatmap (fold change exceeding 1.5X, FDR<0.05). B. Correlation of hyperoxia or mitigation gene signatures (as summed z-scores) using genes expressed in four cohorts of normal human lungs (GSE151052, TCGA LUAD, TCGA LUSC, GTEx lung). Pearson Correlation Coefficient was used, with significance achieved at $p < 0.05$. Black boxes indicate the four correlations shown as scatterplots in Panel C. C. Scatterplots indicating the correlation of the hyperoxia transcriptomic response in WT versus the hyperoxia response in the *Cyp1b1*-null mouse model, or versus the mitigation of the hyperoxia response by genetically modified mouse models *Cyp1a1*-null, *Cyp1a2*-null, or *Cyp1b1*-null. Axes show summed z-scores for the indicated comparison, with each point representing a patient sample from the GTEx human lung cohort.

Processes (GOBP) pathway compendium (Fig. 3A, Supplemental Table 1). Enriched pathways showed a robust hyperoxia response, similar across the WT and the three mouse models *Cyp1a1*-null, *Cyp1a2*-null, *Cyp1b1*-null. However, when evaluating GSEA pathways enriched in the comparisons between the hyperoxia exposure in genetically modified mouse models versus the hyperoxia exposure in WT mice, *Cyp1a*-null and *Cyp1a2*-null associated pathways clustered together, consistent with the previously reported phenotypes [11], and there were clear clusters of either up- or down-regulated pathway specific to the *Cyp1b1*-null mice (Fig. 3B, D). Based on the reported phenotypes (e.g. *Cyp1a1*-null and *Cyp1a2*-null mice showed a more severe phenotype in terms of oxygen injury compared to WT, whereas *Cyp1b1*-null mice showed a less severe phenotype), on the clustering patterns observed based on signature correlations (Fig. 2B and C), and on the enriched GSEA pathways (Fig. 3A), we proposed a potential mechanism explaining the protective effect observed in the *Cyp1b1*-null model. Specifically, the phenotype of *Cyp1b1*-null is likely explained by pathways that are enriched in both WT mice and *Cyp1b1*-null mice after hyperoxia exposure but are partially mitigated in hyperoxia-exposed *Cyp1b1*-null mice compared to hyperoxia-exposed WT mice (Fig. 3B). These pathways are highlighted in Fig. 3C. Analysis of the GSEA enriched pathways revealed 207 pathway candidates possibly explaining the protective effect of *Cyp1b1* loss (Fig. 3C), with 129 increased and 78 decreased pathways after hyperoxia exposure. However, since the *Cyp1b1*-null phenotype is opposite to that of the *Cyp1a1*-null and *Cyp1a2*-null mice, we further excluded the pathways that are also mitigated in either of the *Cyp1a1*-null or *Cyp1a2*-null mice upon exposure to hyperoxia, resulting in a refined collection of 118 pathways (Fig. 3C and D). Overall, we determined 69 positively enriched and 49 negatively enriched pathways after hyperoxia exposure that show potential mitigation only in the *Cyp1b1*-null mice (Fig. 3D). Based on the GOBP taxonomy, we carried out enrichment of taxonomy terms separately in the mitigated pathway based on their direction in the WT mice hyperoxia response (Fig. 3E and F, Supp Figs. 1A and 1B) (significance at FDR<0.25). Mitigated pathways both induced and decreased by hyperoxia enriched for organic substance metabolic processes, but induced pathways showed a preference for nitrogen metabolism, whereas suppressed pathways showed a preference for catabolic or carboxylic acid metabolism.

Based on the candidate pathways involved in mitigation of the hyperoxia exposure effects in *Cyp1b1*-null mice, we conducted validation of gene expression changes using qRT-PCR analysis (Fig. 4A). We chose genes involved either in pathways induced by hyperoxia, such as nucleus or membrane organization, or suppressed by hyperoxia, such as development and catabolic processes (Fig. 4B). We expanded our selection to genes changed in hyperoxia in WT and *Cypb1*-null mice by a fold change of least 1.25x, FDR<0.05. Genes such as 90 kDa heat shock protein (*Hspn90aa1)*, Reticulon 4 (*Rtn4*), C–C motif chemokine ligand 17 (*Ccl17*), and C–C motif chemokine ligand 20 (*Ccl20*) were induced by hyperoxia in both WT and *Cyp1b1*-null mice (Fig. 4B); these genes span hyperoxia-induced pathways including cellular macromolecular complex assembly, response to temperature stimulus, and cellular response to interleukin. Mouse double minute 2 (*Mdm2)* was induced by hyperoxia in both WT and *Cyp1b1*-null mice and is part of several hyperoxia-mediated suppressed pathways, including cardiac chamber morphogenesis and catabolic processes. Homeobox A5 (*Hoxa5*) was suppressed by hyperoxia in both WT and *Cyp1b1*-null mice and is involved in the hyperoxia-suppressed pathway of regulation of vasculature development. Interestingly, cyclin dependent kinase inhibitor 1A (*Cdkn1a*) was induced by hyperoxia in both WT and *Cyp1b1*-null mice but mitigated in *Cyp1b1*-null O_2 mice compared to WT O_2 mice and is a part of hyperoxia-induced pathways (response to temperature stimulus, RAS protein signal transduction, and cellular response to amino acid starvation). The cell cycle pathway was induced by hyperoxia in WT mice and suppressed in all mutant murine models; hence, it was not selected as a *Cyp1b1*-specific mitigation pathway. However, we noticed that *Hoxa*5, *Mdm2*, and *Cdkn1a* were all cell cycle-specific genes mitigated at the transcriptional level, based on microarray data, only in the *Cyp1b1*-null mouse model. We selected another cell cycle gene, Cyclin D1 (*Ccnd1*), mitigated based on the microarray data only in the *Cyp1b1*-null mice and demonstrated that it was induced by hyperoxia in both WT and *Cyp1b1*-null mice but mitigated in *Cyp1b1*-null O_2 mice compared to WT O_2 mice (Fig. 4B).

Using a reverse phase protein array (RPPA) platform, we assessed proteins associated with the 118 mitigated pathways (Fig. 5A). We determined proteins similarly increased by hyperoxia exposure in both WT and *Cyp1b1*-null mice, specifically phospho-AMPK-alpha (T172) and protein patched homolog 1 (PTCH), and similarly decreased by hyperoxia exposure p70S6K (Fig. 5B). Interestingly, we also identified proteins affected by hyperoxia in WT mice but mitigated between *Cyp1b1*-null O_2 mice and WT O_2 mice: eukaryotic translation initiating factor 4E (eIF4E) was induced by hyperoxia in WT then decreased in *Cyp1b1*-null O_2 mice, whereas insulin receptor substrate 1 (IRS1), mammalian target of rapamycin (mTOR), and phosphatase and tensin homolog (PTEN) were decreased by hyperoxia in WT mice but induced in *Cyp1b1*-null O_2 mice (Fig. 5B). Overall, the proteomic validation data indicates a strong association with mitigation of metabolic processes in *Cyp1b1*-null O_2 mice, in particular catabolism and lipid metabolism (Fig. 5A).

3.3. *Hyperoxic responses in WT and cytochrome P450 mutant mice associated with adult and pediatric lung diseases*

As demonstrated numerous times in cancer biology, gene signatures obtained from *in vitro* or *in vivo* experiments can be utilized to mine public disease datasets and interrogate quantitative associations with disease traits, such as cancer vs control or cancer grade/stage [29,31,32]. Recently, our group demonstrated that such approaches are effective outside of the cancer realm, integrating murine hyperoxia gene signatures with BPD blood gene expression profiles [17]. Blood transcriptomics from a human newborn cohort collected at PND14 and PND28 [22] indicated that signatures of hyperoxia exposure in murine lung of either WT or *Cyp1a1*-null, *Cyp1a2*-null, or *Cyp1b1*-null models associated positively with severity of BPD or the need for O_2 supplementation and, conversely, associated negatively with birth weight or gestational age (Fig. 6A). Strikingly, the hyperoxia response of *Cyp1b1*-null mice, but not *Cyp1a1*-null or *Cyp1a2*-null mice, relative to the WT hyperoxia response associated with reduced risk of BPD or oxygen supplementation in d14 BPD samples; the *Cyp1a1*-null hyperoxia treatment positively associated with BPD risk in d28 BPD samples, indicating a further exacerbation of the hyperoxia deleterious effects (Fig. 6A, E). Using an adult human ARDS blood transcriptome cohort GSE32707 [23], hyperoxia exposure signatures in WT or the three mutant mice and hyperoxia mitigation signatures in all three mutant mice showed opposite correlations with risk of progression to ARDS, but did not distinguish between *Cyp1a1*-null, *Cyp1a2*-null, or *Cyp1b1*-null

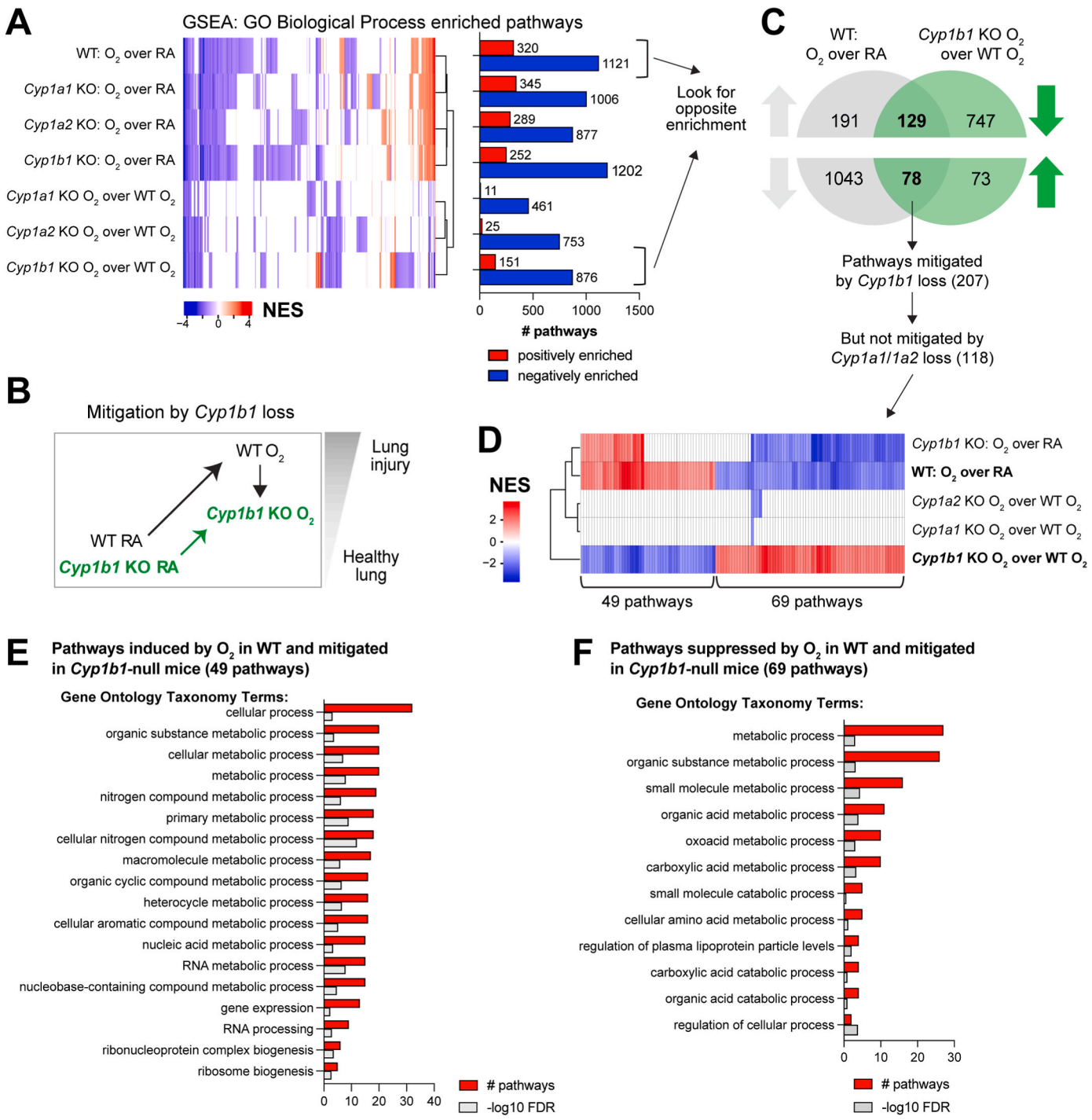

Fig. 3. Use of enriched pathways to dissect a transcriptional program specific to the *Cyp1b1*-null mice mitigating the effects of hyperoxia exposure in WT mice. A. Heatmap with unbiased clustering of enriched pathways by Gene Set Enrichment Analysis (GSEA) from comparisons of hyperoxia response and potential mitigation of hyperoxia effects in mouse models *Cyp1a1*-, *Cyp1a2*-, *Cyp1b1*-null (KO). Number of positively and negatively enriched pathways are shown in bar graph. B. Hypothesized hyperoxia mitigation model in *Cyp1b1*-null mice. C. Venn diagram to identify candidate pathways to explain the mitigation of hyperoxia effects in *Cyp1b1*-null mice, where pathway enrichment is oppositely enriched. D. Pathways mitigated in the *Cyp1b1*-null mice but not in *Cyp1a1*-null or *Cyp1a2*-null mice. E. Top gene ontology enriched terms in the 49 hyperoxia-induced pathway candidates for hyperoxia effects mitigated in the *Cyp1b1*-null mice. F. Top gene ontology enriched terms in the 69 hyperoxia-suppressed pathway candidates for hyperoxia effects mitigated in the *Cyp1b1*-null mice.

(Fig. 6B). Using lung transcriptomics data from The Cancer Genome Atlas, hyperoxia exposure signatures associated with cancer risk in both lung adenocarcinoma (LUAD) [19] and lung squamous carcinoma (LUSC) [20], whereas mutant hyperoxia mitigation signatures showed association with reduced cancer risk for all three *Cyp1a*, *Cyp1a2*, and *Cyp1b1* genes (Fig. 6C). Analysis of both blood and lung transcriptomic cohorts for Idiopathic Pulmonary Fibrosis (IPF) patients showed that whereas hyperoxia exposure associated with IPF risk, hyperoxia mitigation signatures in either *Cyp1a2*-null or *Cyp1b1*-null were associated with reduced IPF risk (Fig. 6D, Supplemental Fig. 2).

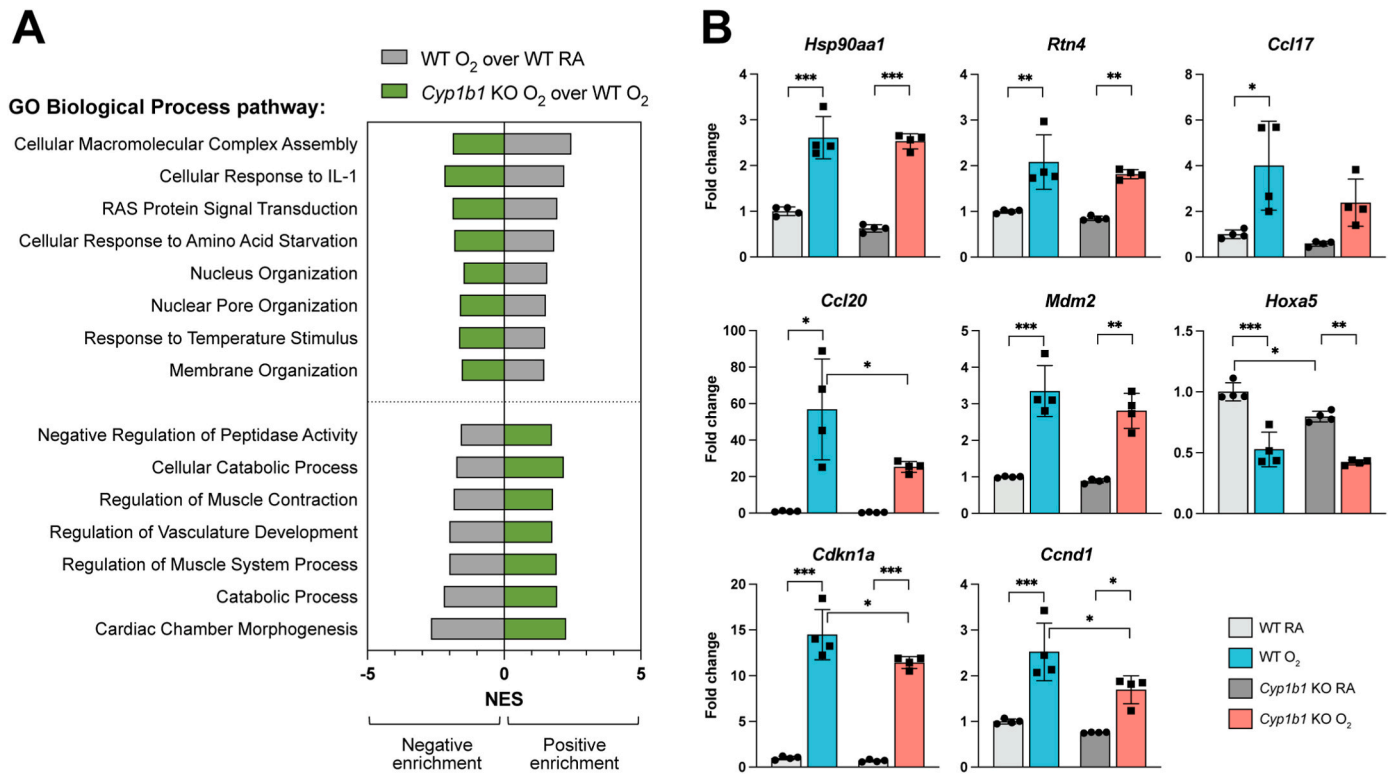

Fig. 4. Gene-level evaluation of hyperoxia exposure responses mitigated in *Cyp1b1*-null mice. A. Selected pathways enriched by hyperoxia in WT (grey bars) and mitigated in *Cyp1b1*-null mice (green bars). B. qRT-PCR to assess mRNA expression of genes involved in a typical hyperoxia response and found in the enriched pathway genesets. Fold change relative to WT normoxia (RA) for each treatment is shown, with asterisks indicating significance (*p < 0.05, **p < 0.005, ***p < 0.0005, ****p < 0.0001). (For interpretation of the references to color in this figure legend, the reader is referred to the Web version of this article.)

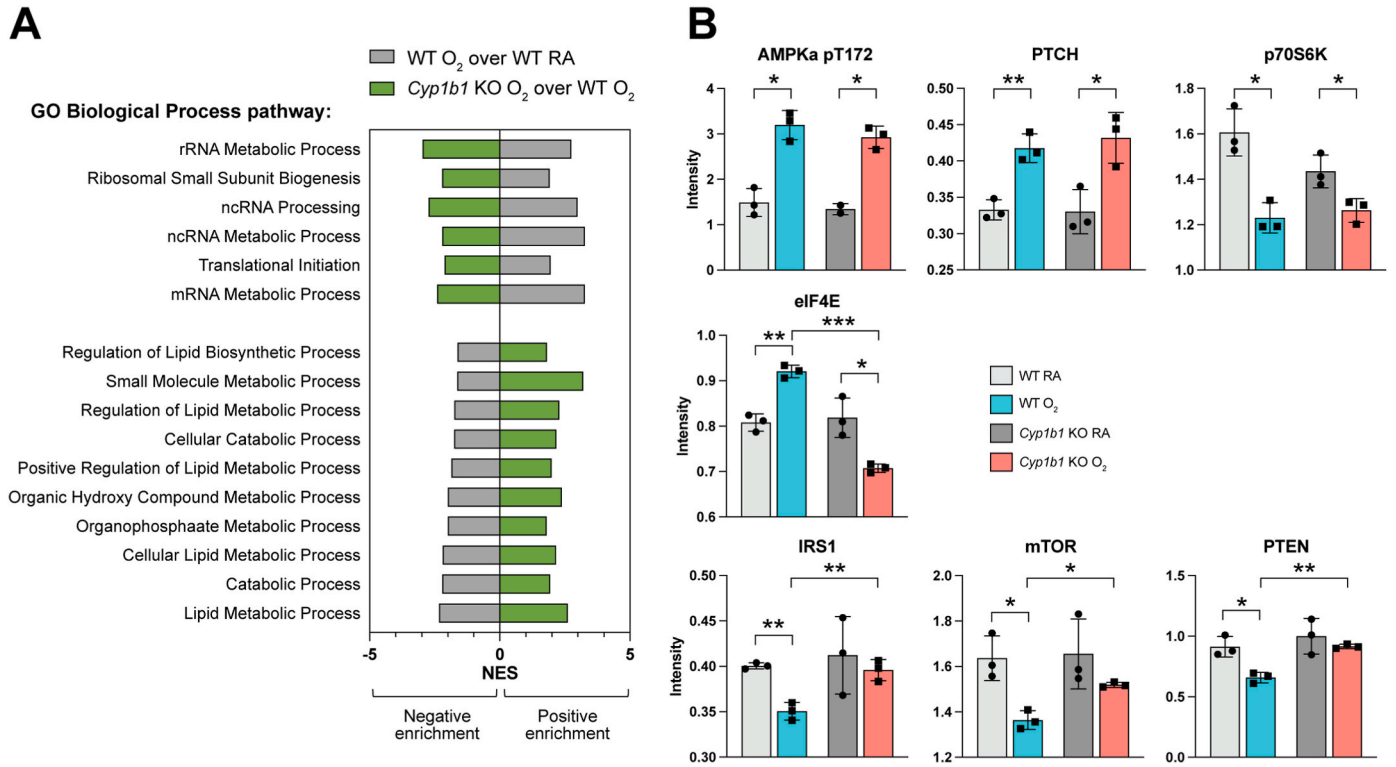

Fig. 5. Protein-level evaluation of hyperoxia exposure responses mitigated in *Cyp1b1*-null mice. A. Selected pathways enriched by hyperoxia in WT (grey bars) and mitigated in *Cyp1b1*-null mice (green bars). B. Reverse Phase Protein Array (RPPA) to assess levels of proteins affected by hyperoxia and found in the enriched pathway genesets. Protein intensity values for each treatment are shown, with asterisks indicating significance (*p < 0.05, **p < 0.005, ***p < 0.0005). (For interpretation of the references to color in this figure legend, the reader is referred to the Web version of this article.)

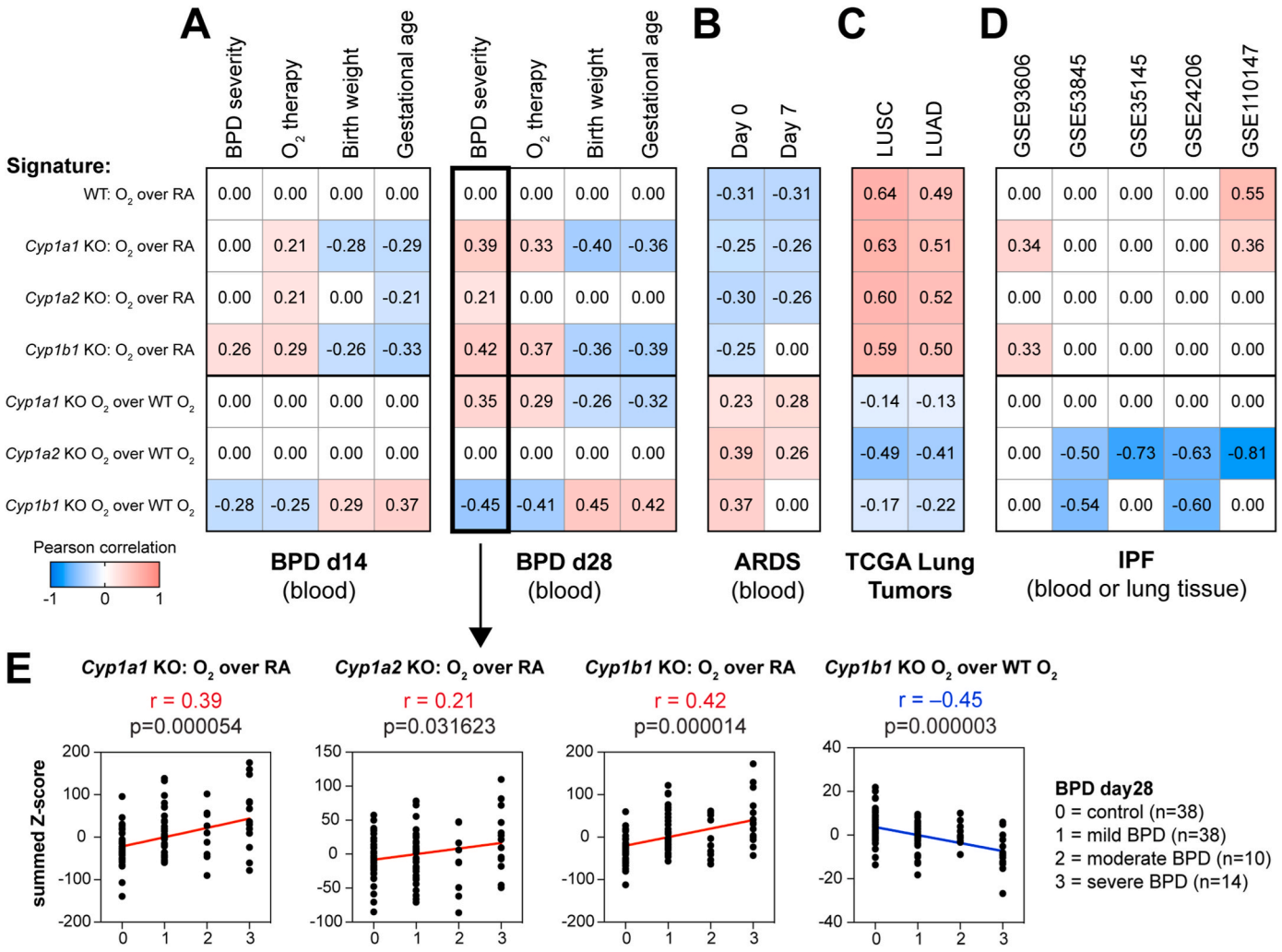

Fig. 6. Clinical associations of disease progression with hyperoxia exposure responses in a wide range of lung disease models were reversed in the *Cyp1b1*-null hyperoxia mitigation signature. Publicly available transcriptomics data from blood or lung tissues were used to perform clinical associations between hyperoxia signatures or hyperoxia mitigation signatures (summed z-scores) and disease progression. Data sets used were (A) Bronchopulmonary dysplasia (BPD) blood transcriptomics from newborns at d14 or d28 (GSE32472), (B) ARDS patient blood samples at d0 and d7 (GSE32707), (C) adenocarcinoma (LUAD) or squamous (LUSC) lung tumor samples from TCGA, and (D) Idiopathic pulmonary fibrosis (IPF) transcriptomics from blood (GSE93606) or lung tissues (GSE53845, GSE35145, GSE24206, and GSE110147). E. Detailed scatterplots from panel A (black boxes) show the association of hyperoxia exposure signatures in *Cyp1a1*-null, *Cyp1a2*-null, or *Cyp1b1*-null mice or the hyperoxia response mitigation signature of *Cyp1b1*-null mice with severity of BPD at d28. Associations were evaluated using the parametric Pearson correlation, with the Pearson correlation coefficient (r) and p-values indicated.

4. Discussion

Several murine studies have demonstrated the protective effects of CYP1B1 enzymes against hyperoxic lung injury [8,33]. The aim of this study was to analyze transcriptomic responses unique to *Cyp1b1*-null mice exposed to hyperoxia that may provide insight into the underlying injury mechanisms contributed by CYP1B1 enzymes in hyperoxic environments. In order to parse through these mechanisms, a systematic approach was developed to analyze differences in pathways, gene expression, and protein levels amongst WT, *Cyp1a1*-, *Cyp1a2*-, and *Cyp1b1*-null mice. Integration with human blood or lung transcriptomics enabled the analysis of our murine hyperoxia gene signatures with those identified in BPD.

The phenotype previously reported by our group is that *Cyp1b1*-null mice exposed to hyperoxia exhibit milder effects compared to WT mice exposed to hyperoxia [10]. To understand that difference, we evaluated the very same comparison at gene signature and enriched pathway level and compared it with the hyperoxia response of WT mice (Fig. 2A). However, following approaches commonly used to tease apart the role of different genotypes in hyperoxia exposure [11,34], we have also analyzed neonatal hyperoxic lung injury compare the hyperoxic response of WT mice to the hyperoxic response of the mutant mice (Fig. 2B and C). Hyperoxia exposure led to changes in gene expression in the same direction but at different extents in WT, *Cyp1a1*-, *Cyp1a2*-, and *Cyp1b1*-null mice. To delineate the potential mechanism by which CYP1B1 enzymes contribute to hyperoxic lung injury, enriched pathways due to transcriptomic responses for WT, *Cyp1a1*-null, *Cyp1a2*-null, and *Cyp1b1*-null mice exposed to both normoxic and hyperoxic environments were analyzed and compared. First, enriched pathways common to both WT and *Cyp1b1*-null mice were removed from consideration. Second, because CYP1A enzymes have shown protective, rather than contributory, effects on hyperoxic lung injury, enriched pathways common to *Cyp1a1*-null, *Cyp1a2*-null, and *Cyp1b1*-null mice were also removed. Out of 207 pathways attenuated in *Cyp1b1*-null mice exposed to hyperoxia, 39 were attenuated in the *Cyp1a1*-null and *Cyp1a2*-null mice as well after hyperoxia exposure; those pathways included six cell cycle related pathways and four apoptotic pathways. However, simple mitigation of a pathway or collection of related pathways is not sufficient to mitigate the hyperoxia phenotypes. Following this analysis, 118 pathways were determined to be either uniquely up- or

down-regulated in *Cyp1b1*-null mice exposed to hyperoxia. Of the 118 pathways identified, 69 decreased and 49 induced pathways by hyperoxia exposure in WT mice were mitigated in *Cyp1b1*-null mice. The induced pathways included nitrogen and folic acid metabolism while decreased pathways demonstrated carboxylic acid, lipid, fatty acid, glutamate, and amino acid metabolism. These unique pathways may give insight into the potential mechanisms by which CYP1B1 enzymes promote hyperoxic lung injury. Accumulation of intracellular nitrogen is toxic to cells [35]. Therefore, mitigation of hyperoxic induction of nitrogen metabolism in *Cyp1b1*-null mice may reduce the accumulation of nitrogen and prevent resulting cellular damage. Promotion of nitrogen accumulation may be one possible mechanism in which CYP1B1 enzymes contribute to hyperoxic lung injury. Conversely, hyperoxia resulted in a decrease in carboxylic acid metabolism in WT mice, which is essential in many phase-I reactions for xenobiotic and endogenous molecular metabolism [36]. *Cyp1b1*-null mice restored carboxylic acid metabolism, indicating that the presence of CYP1B1 enzymes in WT mice may be interfering with carboxylic acid metabolism in the setting of hyperoxia. Therefore, decreased carboxylic acid metabolism may offer another potential mechanism in which CYP1B1 enzymes contribute to lung injury under hyperoxic conditions.

Differences in gene expression between *Cyp1b1*-null and WT O_2 mice were also analyzed to determine other possible mechanisms. Some gene expression alterations caused by hyperoxia were common to both *Cyp1b1*-null and WT mice, such as the induction of *Mdm2* and the suppression of *Hoxa5*. Hyperoxia-driven *Cdkn1a* and *Ccnd1* gene induction was mitigated in *Cyp1b1*-null mice compared to WT mice. Lack of *Ckdn1a* expression has been shown to worsen lung injury secondary to increased cellular apoptosis [37]. *Ccnd1* may have a similar mechanism of action, as it serves as a regulator of CDK kinases, impacting cell cycle progression [38]. Decreased expression of these cell cycle regulators in *Cyp1b1*-null mice may prevent regeneration of damaged lung tissue in the setting of hyperoxic injury in comparison to WT mice.

The elongation factor eIF4E is a crucial component of translation initiation in the process of protein synthesis [39]. Our analysis found that in a hyperoxic environment, eIF4E protein expression was induced in WT mice but decreased in *Cyp1b1*-null mice. Inhibition of this protein has become a key mechanistic target in cancer drug development [39]. Because eIF4E inhibition may prevent cancer development and progression, *Cyp1b1*-null mice may have some level of protection from uncontrolled cellular proliferation due to the decreased eIF4E levels in hyperoxic exposure [40,41]. *Cyp1b1*-null mice also maintained higher expression of the oncogenic protein mTOR and the tumor suppressor protein PTEN after hyperoxia exposure than WT. Because of the contradictory mechanisms of these two proteins, further analysis would need to be conducted to determine the net effect the increased levels have on hyperoxic lung injury in *Cyp1b1*-null mice [42–44].

For further analysis, the gene signatures from these murine models were integrated with human blood or lung transcriptome of pulmonary diseases. The hyperoxic gene signatures of all the murine models, WT, *Cyp1a1*-null, *Cyp1a2*-null, and *Cyp1b1*-null, associated positively with BPD and the need for O_2 supplementation and negatively with birth weight and gestational age. This result indicates that exposure to hyperoxia is a determining factor for BPD, regardless of the presence of CYP1 enzymes. However, an important finding showed that the hyperoxic signature of *Cyp1b1*-null mice had a reduced risk of BPD and oxygen supplementation, while *Cyp1a1*-null and *Cyp1a2*-null mice hyperoxic signatures did not demonstrate this association. Hyperoxia response gene signatures in WT, *Cyp1a1*-null, *Cyp1a2*-null, and *Cyp1b1*-null mice correlated strongly with transcriptome dysregulation seen in other lung diseases, such as ARDS, lung cancer or IPF, and conversely hyperoxia gene expression for each mouse mutant compared to WT associated with lower disease risk; however, there was no risk reduction specific to *Cyp1b1*-null mice as seen for BPD. These results further validate the hypothesis that CYP1B1 enzymes contribute to hyperoxic lung injury.

5. Conclusion

In conclusion, our analysis provides insight into possible mechanisms by which CYP1B1 enzymes contribute to hyperoxic lung injury. Based on these results, CYP1B1 enzymes may lead to nitrogen accumulation and interfere with carboxylic acid metabolism in hyperoxic environments, which can be toxic to cells. Furthermore, CYP1B1 enzymes may play a role in the induction of *Cdkna1* and *Ccnd1* transcription under hyperoxic conditions, allowing for continued proliferation of damaged cells and further contributing to lung injury. Similarly, induction of the transcription initiating protein eIF4E may also allow for continued proliferation in this setting. More studies are required to analyze these identified pathways unique to the *Cyp1b1*-null model in order to further understand the mechanistic interactions of these pathways as well as to identify potential targets for therapy to treat or prevent pulmonary disease development in hyperoxic settings.

Declaration of competing interest

The authors declare that they have no known competing financial interests or personal relationships that could have appeared to influence the work reported in this paper.

Data availability

Data will be made available on request.

Acknowledgements

SLG, MJR, TG, and CC were partially funded by The Cancer Prevention and Research Institute of Texas (CPRIT) RP170005 and RP210227, NIH/NCI P30 shared resource grant CA125123, NIH/NIEHS grants P30 ES030285, and NIMHD P50MD015496. KL was supported by R01HL144775 and R01HL146395. BM was supported by 1P42 ES0327725, R01HL129794, 1R01ES029382, 1R21ES032739.

Appendix A. Supplementary data

Supplementary data to this article can be found online at https://doi.org/10.1016/j.redox.2023.102790.

References

[1] T. Duke, S.M. Graham, M.N. Cherian, et al., Oxygen is an essential medicine: a call for international action, Int. J. Tubercul. Lung Dis. 14 (11) (2010) 1362–1368.
[2] R.H. Kallet, M.A. Matthay, Hyperoxic acute lung injury, Respir. Care 58 (1) (2013) 123–141.
[3] R. Stading, X. Couroucli, K. Lingappan, et al., The role of cytochrome P450 (CYP) enzymes in hyperoxic lung injury, Expet Opin. Drug Metabol. Toxicol. 17 (2) (2021) 171–178.
[4] W.J. Wiersinga, A. Rhodes, A.C. Cheng, et al., Pathophysiology, transmission, diagnosis, and treatment of coronavirus disease 2019 (COVID-19): a review, JAMA 324 (8) (2020) 782–793.
[5] X.I. Couroucli, Y.H. Liang, W. Jiang, et al., Prenatal administration of the cytochrome P4501A inducer, Beta-naphthoflavone (BNF), attenuates hyperoxic lung injury in newborn mice: implications for bronchopulmonary dysplasia (BPD) in premature infants, Toxicol. Appl. Pharmacol. 256 (2) (2011) 83–94.
[6] R.G. Brower, P.N. Lanken, N. MacIntyre, et al., Higher versus lower positive end-expiratory pressures in patients with the acute respiratory distress syndrome, N. Engl. J. Med. 351 (4) (2004) 327–336.
[7] I.-R. Investigators, A. the, New Zealand Intensive Care Society Clinical Trials G, et al. Conservative Oxygen Therapy during Mechanical Ventilation in the ICU, N. Engl. J. Med. 382 (11) (2020) 989–998.
[8] A. Veith, B. Moorthy, Role of cytochrome P450s in the generation and metabolism of reactive oxygen species, Curr Opin Toxicol 7 (2018) 44–51.
[9] U.M. Zanger, M. Schwab, Cytochrome P450 enzymes in drug metabolism: regulation of gene expression, enzyme activities, and impact of genetic variation, Pharmacol. Ther. 138 (1) (2013) 103–141.
[10] A.C. Veith, B. Bou Aram, W. Jiang, et al., Mice lacking the cytochrome P450 1B1 gene are less susceptible to hyperoxic lung injury than wild type, Toxicol. Sci. 165 (2) (2018) 462–474.

[11] K. Lingappan, S. Maity, W. Jiang, et al., Role of cytochrome P450 (CYP)1A in hyperoxic lung injury: analysis of the transcriptome and proteome, Sci. Rep. 7 (1) (2017) 642.
[12] J.T. Buters, S. Sakai, T. Richter, et al., Cytochrome P450 CYP1B1 determines susceptibility to 7, 12-dimethylbenz[a]anthracene-induced lymphomas, Proc. Natl. Acad. Sci. U. S. A. 96 (5) (1999) 1977–1982.
[13] P. Du, W.A. Kibbe, S.M. Lin, lumi: a pipeline for processing Illumina microarray, Bioinformatics 24 (13) (2008) 1547–1548.
[14] M.E. Ritchie, B. Phipson, D. Wu, et al., Limma powers differential expression analyses for RNA-sequencing and microarray studies, Nucleic Acids Res. 43 (7) (2015) e47.
[15] A. Subramanian, P. Tamayo, V.K. Mootha, et al., Gene set enrichment analysis: a knowledge-based approach for interpreting genome-wide expression profiles, Proc. Natl. Acad. Sci. U. S. A. 102 (43) (2005) 15545–15550.
[16] Z. Ju, W. Liu, P.L. Roebuck, et al., Development of a robust classifier for quality control of reverse-phase protein arrays, Bioinformatics 31 (6) (2015) 912–918.
[17] S.L. Grimm, X. Dong, Y. Zhang, et al., Effect of sex chromosomes versus hormones in neonatal lung injury, JCI Insight 6 (13) (2021).
[18] S. Durinck, Y. Moreau, A. Kasprzyk, et al., BioMart and Bioconductor: a powerful link between biological databases and microarray data analysis, Bioinformatics 21 (16) (2005) 3439–3440.
[19] N. Cancer Genome Atlas Research, Comprehensive molecular profiling of lung adenocarcinoma, Nature 511 (7511) (2014) 543–550.
[20] N. Cancer Genome Atlas Research, Comprehensive genomic characterization of squamous cell lung cancers, Nature 489 (7417) (2012) 519–525.
[21] G.T. Consortium, D.A. Laboratory, G. Coordinating Center -Analysis Working, et al., Genetic effects on gene expression across human tissues, Nature 550 (7675) (2017) 204–213.
[22] J.J. Pietrzyk, P. Kwinta, E.J. Wollen, et al., Gene expression profiling in preterm infants: new aspects of bronchopulmonary dysplasia development, PLoS One 8 (10) (2013), e78585.
[23] T. Dolinay, Y.S. Kim, J. Howrylak, et al., Inflammasome-regulated cytokines are critical mediators of acute lung injury, Am. J. Respir. Crit. Care Med. 185 (11) (2012) 1225–1234.
[24] P.L. Molyneaux, S.A.G. Willis-Owen, M.J. Cox, et al., Host-microbial interactions in idiopathic pulmonary fibrosis, Am. J. Respir. Crit. Care Med. 195 (12) (2017) 1640–1650.
[25] D.J. DePianto, S. Chandriani, A.R. Abbas, et al., Heterogeneous gene expression signatures correspond to distinct lung pathologies and biomarkers of disease severity in idiopathic pulmonary fibrosis, Thorax 70 (1) (2015) 48–56.
[26] Y.Y. Sanders, N. Ambalavanan, B. Halloran, et al., Altered DNA methylation profile in idiopathic pulmonary fibrosis, Am. J. Respir. Crit. Care Med. 186 (6) (2012) 525–535.
[27] E.B. Meltzer, W.T. Barry, T.A. D'Amico, et al., Bayesian probit regression model for the diagnosis of pulmonary fibrosis: proof-of-principle, BMC Med. Genom. 4 (2011) 70.
[28] M.J. Cecchini, K. Hosein, C.J. Howlett, et al., Comprehensive gene expression profiling identifies distinct and overlapping transcriptional profiles in non-specific interstitial pneumonia and idiopathic pulmonary fibrosis, Respir. Res. 19 (1) (2018) 153.
[29] C. Geng, K. Rajapakshe, S.S. Shah, et al., Androgen receptor is the key transcriptional mediator of the tumor suppressor SPOP in prostate cancer, Cancer Res. 74 (19) (2014) 5631–5643.
[30] B.S. Taylor, N. Schultz, H. Hieronymus, et al., Integrative genomic profiling of human prostate cancer, Cancer Cell 18 (1) (2010) 11–22.
[31] C. Geng, S. Kaochar, M. Li, et al., SPOP regulates prostate epithelial cell proliferation and promotes ubiquitination and turnover of c-MYC oncoprotein, Oncogene 36 (33) (2017) 4767–4777.
[32] H.A. Abbas, N.H.B. Bui, K. Rajapakshe, et al., Distinct TP63 isoform-driven transcriptional signatures predict tumor progression and clinical outcomes, Cancer Res. 78 (2) (2018) 451–462.
[33] D. Dinu, C. Chu, A. Veith, et al., Mechanistic role of cytochrome P450 (CYP)1B1 in oxygen-mediated toxicity in pulmonary cells: a novel target for prevention of hyperoxic lung injury, Biochem. Biophys. Res. Commun. 476 (4) (2016) 346–351.
[34] C. Coarfa, Y. Zhang, S. Maity, et al., Sexual dimorphism of the pulmonary transcriptome in neonatal hyperoxic lung injury: identification of angiogenesis as a key pathway, Am. J. Physiol. Lung Cell Mol. Physiol. 313 (6) (2017) L991–L1005.
[35] D. Zou, J. Li, Q. Fan, et al., Reactive oxygen and nitrogen species induce cell apoptosis via a mitochondria-dependent pathway in hyperoxia lung injury, J. Cell. Biochem. 120 (4) (2019) 4837–4850.
[36] C. Skonberg, J. Olsen, K.G. Madsen, et al., Metabolic activation of carboxylic acids, Expet Opin. Drug Metabol. Toxicol. 4 (4) (2008) 425–438.
[37] J. Blazquez-Prieto, C. Huidobro, I. Lopez-Alonso, et al., Activation of p21 limits acute lung injury and induces early senescence after acid aspiration and mechanical ventilation, Transl. Res. 233 (2021) 104–116.
[38] J.W. Kim, C.K. Rhee, T.J. Kim, et al., Effect of pravastatin on bleomycin-induced acute lung injury and pulmonary fibrosis, Clin. Exp. Pharmacol. Physiol. 37 (11) (2010) 1055–1063.
[39] A. Romagnoli, M. D'Agostino, C. Ardiccioni, et al., Control of the eIF4E activity: structural insights and pharmacological implications, Cell. Mol. Life Sci. 78 (21–22) (2021) 6869–6885.
[40] J. Gao, L. Teng, S. Yang, et al., MNK as a potential pharmacological target for suppressing LPS-induced acute lung injury in mice, Biochem. Pharmacol. 186 (2021), 114499.
[41] X. Li, C. Shan, Z. Wu, et al., Emodin alleviated pulmonary inflammation in rats with LPS-induced acute lung injury through inhibiting the mTOR/HIF-1alpha/VEGF signaling pathway, Inflamm. Res. 69 (4) (2020) 365–373.
[42] H. Populo, J.M. Lopes, P. Soares, The mTOR signalling pathway in human cancer, Int. J. Mol. Sci. 13 (2) (2012) 1886–1918.
[43] H. Hua, Q. Kong, H. Zhang, et al., Targeting mTOR for cancer therapy, J. Hematol. Oncol. 12 (1) (2019) 71.
[44] C.Y. Chen, J. Chen, L. He, et al., PTEN: tumor suppressor and metabolic regulator, Front. Endocrinol. 9 (2018) 338.